

A MECHANISM OF TURBULENT HEAT TRANSFER IN LIQUID METALS

N. Z. AZER† and B. T. CHAO‡

†University of Alexandria, UAR (Egypt) and ‡University of Illinois, Urbana, Ill.

(Received April 1959; revised 15 February 1960)

Abstract—A simplified mechanism of turbulent heat transfer, based on a modification of Prandtl's mixing-length hypothesis, has been proposed. It is assumed that there is a continuous change of momentum and energy during the flight of the eddy. Two expressions giving the ratio of eddy diffusivities for heat and momentum were obtained for fully developed pipe flow. One is for fluids of Prandtl number ranging from 0.6 to 15 and the other for liquid metals. Both correctly predict the influence of Reynolds number, Prandtl number and radial location across the pipe on the diffusivity ratio when compared to trends revealed by limited published data.

Computation of Nusselt number and temperature profile in liquid metals were carried out under conditions of constant wall flux using the deduced expression for diffusivity ratio. They agree well with experimental results. For practical calculation of film coefficient of heat transfer, the following interpolation formula may be used:

$$N_{Nu} = 7 + 0.05 N_{Pr}^{0.25} N_{Pe}^{0.77}$$

which fits the calculated data with a maximum deviation of less than 12 per cent for $N_{Pr} < 0.1$ and $N_{Pe} < 15,000$. Limiting values of Nusselt number as $N_{Pr} \rightarrow 0$ and $N_{Re} \rightarrow \infty$ were discussed.

Résumé—Un mécanisme simplifié de la transmission de chaleur turbulente, fondé sur une modification de l'hypothèse de Prandtl sur la longueur de mélange, est proposé. On suppose qu'il y a une variation continue de la quantité de mouvement et d'énergie pendant la trajectoire de la masse tourbillonnaire. Deux expressions donnent le rapport des diffusivités turbulentes pour la chaleur et la quantité de mouvement ont été obtenues dans le cas d'un écoulement pleinement établi dans une conduite. L'une est valable pour les fluides dont le nombre de Prandtl varie de 0,6 à 15 et l'autre convient pour les métaux liquides. Ces deux expressions permettent de prévoir correctement l'influence du nombre de Reynolds, du nombre de Prandtl et de la distance à l'axe de la conduite sur le rapport des diffusivités, comparativement aux tendances indiquées par les quelques résultats publiés.

Le calcul du nombre de Nusselt et du profil des températures dans les métaux liquides a été effectué, dans les conditions de flux de paroi constant, en se servant de l'expression obtenue pour le rapport des diffusivités. Ce calcul est en bon accord avec les résultats expérimentaux. Pour le calcul pratique d'un coefficient de transmission de chaleur surfacique, on peut utiliser la formule d'interpolation suivante

$$N_{Nu} = 7 + 0,05 N_{Pr}^{0,25} N_{Pe}^{0,77}$$

qui donne les résultats calculés avec un écart maximum inférieur à 12% pour $0,1 < N_{Pr} < 15.000$. Les valeurs limites du nombre de Nusselt quand $N_{Pr} \rightarrow 0$ et $N_{Pe} \rightarrow \infty$ sont discutées.

Zusammenfassung—Für die turbulente Wärmeübertragung wird ein vereinfachter Mechanismus vorgeschlagen, der auf einer Abwandlung der Hypothese der Mischungslänge nach Prandtl beruht. Es wird angenommen, dass sich während der Bewegung eines Ballens Impuls und Energie kontinuierlich ändern. Für voll entwickelte Rohrströmung erhält man zwei Ausdrücke für das Verhältnis der turbulenten Leitfähigkeiten für Wärme und Impuls, einen für den Bereich der Prandtlzahl von 0,6 bis 15 und den anderen für flüssige Metalle. Beide geben den Einfluss der Reynoldszahl, der Prandtlzahl und der radialen Koordinate im Rohr auf das Verhältnis der Wärmeleitfähigkeiten richtig wieder, wenn man sie mit Literaturwerten vergleicht.

Nusseltzahlen und Temperaturprofile für flüssige Metalle wurden unter der Bedingung konstanter Wärmestromdichte an der Wand berechnet, wobei der abgeleitete Ausdruck für das Verhältnis der Leitfähigkeiten verwendet wurde. Die Ergebnisse stimmen gut mit Messungen überein. Für die praktische Berechnung kann folgende Gleichung verwendet werden.

$$N_{Nu} = 7 + 0,05 N_{Pr}^{0,25} N_{Pe}^{0,77}$$

Diese Gleichung gibt die errechneten Werte mit einer Größenabweichung von weniger als 12% $N_{Pr} < 0,1$ und $N_{Pe} < 15000$. Auch die Grenzwerte der Nusseltzahl für $N_{Pr} \rightarrow 0$ und $N_{Re} \rightarrow \infty$ werden diskutiert.

Abstract—Предлагается упрощенный механизм турбулентного теплообмена, основанный на видоизменённой гипотезе Прандтля о длине смешения. Допускается, что происходит непрерывное изменение количества движения и энергии за время движения вихря. Для стабилизированного потока в трубе получены два соотношения между коэффициентом диффузии вихря при переносе тепла и количеством движения. Оба выражения правильно отображают влияние критериев Рейнольдса, Прандтля и радиальной координаты, что и подтверждается сравнением с имеющимися опубликованными данными.

Вычисление критерия Нуссельта и температурного профиля в жидких металлах проводилось в условиях постоянного потока тепла на стенке с использованием соотношения коэффициентов диффузии вихря. Эти данные хорошо согласуются с результатами эксперимента. Для практического расчёта коэффициента теплообмена можно использовать следующую интерполяционную формулу

$$N_{Nu} = 7 + 0,05 N_{Pr}^{0,25} N_{Pe}^{0,77}$$

которая даёт меньше отклонения чем 12% для $N_{Pe} < 0,1$ и $N_{Pe} < 15000$. Рассмотрены предельные значения критерия Нуссельта при $N_{Pr} \rightarrow 0$ и $N_{Re} \rightarrow \infty$.

NOMENCLATURE

a ,	radius of the eddy (ft);	ϵ_M ,	eddy diffusivity for momentum transfer (ft ² /hr);
A ,	area per unit length of pipe (ft ² /ft);	κ ,	thermal diffusivity of fluid, = $k/c_p\rho$ (ft ² /hr);
c_p ,	specific heat at constant pressure (B.t.u./lb °F);†	μ ,	dynamic viscosity of fluid (lb/ft hr);
D ,	pipe inside diameter, $2r_w$ (ft);	ν ,	kinematic viscosity of fluid (ft ² /hr);
g_c ,	mass unit conversion constant (lb ft/Lb hr ²);†	ρ ,	density of fluid (lb/ft ³);
h ,	surface conductance (B.t.u./hr ft ² °F);	τ ,	shear stress at any radius r (Lb/ft ²);
k ,	thermal conductivity of fluid (B.t.u./hr ft °F);	θ ,	time (hr).
l ,	mixing length (ft);	Dimensionless quantities	
q ,	rate of radial heat flow at any radius r per unit length of pipe (B.t.u./hr ft);	b ,	empirical constant in equations (17) and (20);
r ,	radius (ft);	f ,	Darcy friction factor;
r_w ,	inside radius of pipe (ft);	N_{Nu} ,	Nusselt number, hD/k ;
t ,	fluid temperature (°F);	N_{Pe} ,	Peclet number, $N_{Re} N_{Pr} = u_b D/\kappa$;
u ,	axial velocity (ft/hr);	N_{Pr} ,	Prandtl number, $c_p\mu/k = \nu/\kappa$;
u_b ,	mean velocity in pipe (ft/hr);	N_{Re} ,	Reynolds number, $u_b D/\nu$;
v' ,	fluctuating velocity in radial direction (ft/hr);	N_{St} ,	Stanton number, $N_{Nu}/N_{Re}N_{Pr} = h/c_p\rho u_b$;
v^* ,	friction velocity defined by $v^* = \sqrt{(g_c\tau_w/\rho)}$ (ft/hr);	$N_{Pe'}$,	$N_{Re'}$, $N_{St'}$ refer to eddy;
y ,	radial distance from pipe wall (ft);	U	= u/u_b ;
ϵ_H ,	eddy diffusivity for heat transfer (ft ² /hr);	u^+	= u/v^* ;
		y^+ ,	friction distance parameter defined by $y^+ = v^*y/\nu$;
		Z	= r/r_w ;
		a	= ϵ_H/ϵ_M , ratio of eddy diffusivity of heat to momentum;

† Lb represents pounds force, and lb pounds mass in this paper.

Subscripts

- b*, bulk;
- c*, center of pipe;
- e*, eddy;
- w*, wall.

Other symbols or subscripts that might be used are defined in the text.

1. INTRODUCTION

THE advantage of using liquid metals as heat-transfer media is primarily due to their high conductivity, relatively low viscosity and high boiling point. Among the disadvantages, one may mention the difficulty of handling. Some liquid metals are corrosive and chemically reactive. Techniques are being developed to overcome these difficulties.

After the World War II, a widespread interest has appeared in using liquid metals as a coolant in nuclear-chain reactors. In spite of the many attractions and the potentialities of its use in industrial applications, the mechanism of turbulent heat transfer, even under the simple condition of fully developed pipe flow, is not well understood. Lubarsky and Kaufman [1] made a thorough examination and re-evaluation of the experimental results on film coefficient of heat transfer reported by numerous investigators up to 1953. They observed that the bulk of data for Nusselt number were lower than those predicted by the then existing theoretical analyses. After reviewing the available literature on the subject, and performing some preliminary analysis, the writers were led to believe that a major reason for the observed discrepancy could be due to the oversimplified relation commonly assumed for eddy diffusivities of heat and momentum. An improved macroscopic theory of turbulent exchange mechanism is herein proposed which brings closer the theoretical predictions and measured data, both for heat-transfer coefficients and temperature profiles.

The governing equations for the analysis of turbulent heat transfer in circular tubes, at a large distance from the entrance, where both the velocity and temperature profiles are fully developed,† may be expressed as:

$$\frac{\tau g_c}{\rho} = (\nu + \epsilon_M) \frac{du}{dy} \tag{1}$$

$$\frac{q}{Ac_p \rho} = -(\kappa + \epsilon_H) \frac{dt}{dy} \tag{2}$$

Equations (1) and (2) are deduced from the time averaged Reynolds momentum and energy equation for axially symmetric incompressible flow in a pipe, using the following assumptions:

- (a) The flow is steady on the average.
- (b) All properties are constants.
- (c) Axial conduction is negligible when compared to axial convection.‡
- (d) Frictional heating is negligible.

The analogous nature of momentum transfer and heat transfer is evident from the foregoing pair of equations. They are linked to each other through the relationship between the two eddy diffusivities. Such a relation depends on the physical model which one selects.

Reynolds [4], who made the first important step in the analysis of turbulent exchange mechanism, postulated that energy and momentum were transferred in the same manner. Reynolds analogy, as the postulate is commonly known, implies $\epsilon_H = \epsilon_M$. Taylor [5], Prandtl [6], von Kármán [7], Martinelli [8, 9], Lyon [10] and others [2, 11, 12] all adopted this assumption in their analysis of turbulent heat transfer. Relatively recently, various experiments have been conducted to determine the diffusivity ratio *a* from measured temperature and velocity profiles in fluids flowing turbulently in circular tubes as well as between parallel plates [13-21]. It has been established that *a* is not a constant and, with even more certainty, ϵ_H cannot in general be equal to ϵ_M . In spite of the discrepancies which exist among the published data, it appears that the following has generally been agreed on:

- (a) The diffusivity ratio, *a*, is not a constant across the tube.
- (b) For air, *a* is greater than unity. It exhibits higher values in regions close to the wall and has

† Seban and Shimazaki's definition of fully developed temperature profile is implied, see [2].

‡ Schneider [3] has demonstrated that this is a good assumption provided that $N_{Pe} > 100$.

a decreasing trend toward the pipe center. For flow at high subsonic Mach numbers, an opposite trend has been reported [21]. The latter may be attributed to compressibility. Increasing N_{Re} tends to reduce α but in no case is it less than unity.

(c) For liquid metals, α is less than unity. The variation of α with a greater distance from the wall shows a trend opposite to that described in (b) above. At a fixed N_{Re} , α increases first relatively rapidly and then more slowly as one moves away from the wall. Increasing N_{Re} tends to increase α but in no case it is greater than unity.

Jenkins [22], Deissler [23] and recently Lykoudis and Touloukian [24] attempted to evaluate α on a theoretical basis by modifying Prandtl's mixing-length theory. All the models proposed failed to predict the behavior of α as summarized above.

2. SUGGESTED MODEL FOR THE MECHANISM OF TURBULENT EXCHANGE—MODIFIED MIXING-LENGTH THEORY

In 1925, Prandtl [25] proposed the now famous mixing-length hypothesis. It was presumed that the eddy preserved both its momentum and energy while travelling between layers of a fluid before mixing occurs. Referring to Fig. 1(a), an eddy originated at layer (1) and moving upwards preserved its velocity u_1 and temperature t_1 over an average distance l called the mixing-length till it reached layer (2) where it mixes with the bulk of fluid there and completely loses its identity. An eddy created at layer (2) and moving downwards behaves in a similar way as illustrated in Fig. 1(b). Conceivably, neither the momentum (in the u -direction) nor the energy may be conserved during its travel. In fluids of high thermal conductivity, heat transfer at the surface of the eddy may become appreciable. Thus in Fig. 2(a), an eddy created at layer (1), with velocity u_1 and temperature t_1 will attain a velocity u'_1 and temperature t'_1 before mixing takes place at layer (2). A similar event takes place for an eddy moving towards the wall as illustrated in Fig. 2(b). With this simple modifi-

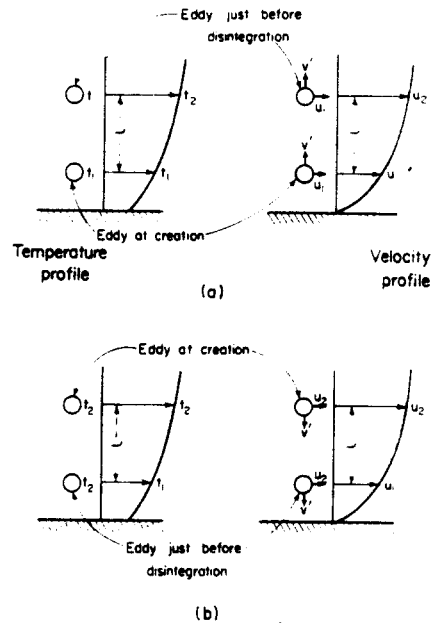


FIG. 1. Prandtl's model of turbulent mixing: (a) eddy moving upward; (b) eddy moving downward.

cation of Prandtl's mixing-length hypothesis, one has:

$$\begin{aligned} \frac{\epsilon_H}{\epsilon_M} &= \frac{(t_2 - t'_1)/(t_2 - t_1)}{(u_2 - u'_1)/(u_2 - u_1)} \\ &= \frac{1 + (u'_1 - u_1)/(u_2 - u'_1)}{1 + (t'_1 - t_1)/(t_2 - t'_1)} \end{aligned}$$

for an eddy moving upward (3a†)

and

$$\begin{aligned} \frac{\epsilon_H}{\epsilon_M} &= \frac{(t'_2 - t_1)/(t_2 - t_1)}{(u'_2 - u_1)/(u_2 - u_1)} \\ &= \frac{1 + (u_2 - u'_2)/(u'_2 - u_1)}{1 + (t_2 - t'_2)/(t'_2 - t_1)} \end{aligned}$$

for an eddy moving downward (3b)†

In order to maintain continuity, one would logically assume that there will be just as many eddies moving upward as there are moving downward. (Equations (3a) and (3b) are, in effect, identical.)

† See (33) for derivation.

In the foregoing equations, $(u_2 - u_1')$ and $(t_2 - t_1')$ are conceived, respectively, as the fluctuating axial component of velocity and temperature at layer (2). The corresponding fluctuating quantities at layer (1) are $(u_2 - u_1)$ and $(t_2' - t_1)$.

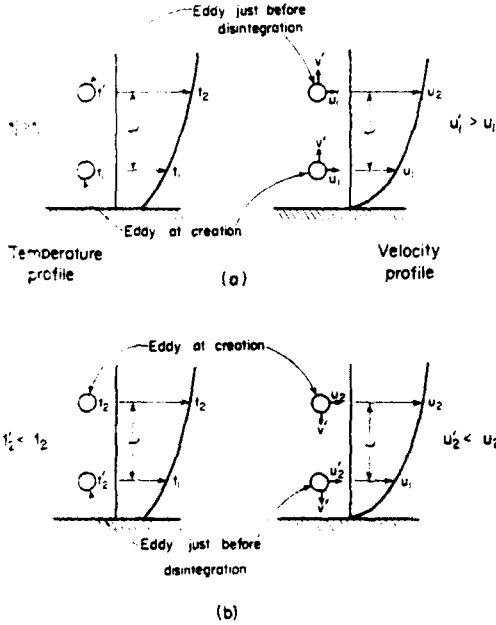


Fig. 2. Modified Prandtl's model of turbulent mixing: (a) eddy moving upward; (b) eddy moving downward.

To ascertain the influence of fluid drag and heat transfer at the surface of the eddy, it is assumed that they are both associated with its boundary layer. For simplicity, the eddy is presumed to be spherical. As it moves from layer (1) to layer (2), its average axial velocity is $\frac{1}{2}(u_1 + u_1')$ while that of the surrounding fluid is $\frac{1}{2}(u_2 + u_1)$. Application of the momentum principle yields,

$$\lambda \frac{\rho}{2} \left(\frac{u_2 - u_1'}{2} \right)^2 S \frac{l}{v} = \rho V (u_1' - u_1) \quad (4)$$

S being the surface area of the eddy, V its volume, l/v , the time required for an eddy to travel between layers (1) and (2) and λ the average friction coefficient defined by:

$$\begin{aligned} \lambda &= \frac{\tau_e g_c}{\frac{1}{2} \rho \left[\frac{1}{2}(u_2 + u_1) - \frac{1}{2}(u_1 + u_1') \right]^2} \\ &= \frac{\tau_e g_c}{\frac{1}{2} \rho \left[\frac{1}{2}(u_2 - u_1') \right]^2} \end{aligned}$$

For spherical eddy of radius a , $V/S = a/3$. Equation (4), upon rearrangement, becomes

$$\frac{u_1' - u_1}{u_2 - u_1'} = \frac{3}{2} \lambda \left(\frac{l}{a} \right) \frac{u_2 - u_1'}{4v'} \quad (5)$$

To estimate the amount of heat transfer during flight, the spherical eddy is conceived to have an average temperature $T_e [= \frac{1}{2}(t_1 + t_1')]$ being immersed in an immense fluid initially at a uniform temperature $T_0 [= \frac{1}{2}(t_1 + t_2)]$. The film coefficient of heat transfer at the eddy surface is h_e . We shall now proceed to evaluate the heat transferred from the surrounding fluid to the eddy during the flight time l/v' . With this simplified model,† the differential equation of the temperature field in the surrounding fluid and its initial and boundary conditions are as follows:

$$T_\theta = \kappa \left(T_{RR} + \frac{2}{R} T_R \right), a < R < \infty$$

$$T(0, R) = T_0; T_R(\theta, a)$$

$$= -h' [T_e - T(\theta, a)], h' = \frac{h_e}{k} \quad (6) \ddagger$$

The solution of equation (6) is

$$\left. \begin{aligned} \frac{T - T_0}{T_e - T_0} &= \frac{a}{R} \frac{ah'}{1 + ah'} \left\{ 1 - \right. \\ &- \operatorname{erf} \left[\frac{R - a}{2\sqrt{(\kappa\theta)}} \right] - \exp [H(R - a) + H^2\kappa\theta] \times \\ &\times \operatorname{erfc} \left[\frac{R - a}{2\sqrt{(\kappa\theta)}} + H\sqrt{(\kappa\theta)} \right] \left. \right\} \end{aligned} \right\} (7)$$

where

$$H = \frac{1 + ah'}{a} \quad (7a)$$

† An alternative model would be to assume that the surrounding fluid is at a constant, uniform temperature T_0 and to calculate the total heat transferred during the time l/v , allowing the temperature of the eddy to vary.

‡ $T_\theta = \frac{\partial T}{\partial \theta}$, $T_R = \frac{\partial T}{\partial R}$ etc.

The quantity of heat flowing into the eddy during the flight time l/v' is

$$Q_e = \int_0^l k(4\pi a^2) T_R(\theta, a) d\theta = k(4\pi a^2) (T_0 - T_e) \frac{h'}{1 + ah'} \left[\frac{l}{v'} + \frac{aH - 1}{\kappa H^2} F(X) \right] \quad (8)$$

$$\text{where } F(X) = \exp(X^2) \operatorname{erfc} X + \frac{2}{\sqrt{\pi}} X - 1 \quad (8a)$$

$$\text{and } X = H \sqrt{\left(\kappa \frac{l}{v'} \right)} \quad (8b)$$

This flow of heat results in an enthalpy change of the eddy and is reflected as a temperature increase,

$$t'_1 - t_1 = \frac{Q_e}{\frac{4}{3}\pi a^3 c_p \rho} \quad (9)$$

Since $T_0 - T_e = \frac{1}{2}(t_2 - t'_1)$, one obtains from equation (9):

$$\frac{t'_1 - t_1}{t_2 - t'_1} = \frac{3\kappa}{2a} \frac{h'}{1 + ah'} \left[\frac{l}{v'} + \frac{aH - 1}{\kappa H^2} F(X) \right] \quad (10)$$

Equation (10) contains the surface coefficient of the eddy h_e which has yet to be evaluated. According to the proposed model, the heat transfer is characterized by the laminar boundary layer at the eddy surface. Possible influences of curvature behind it are to be ignored, and Pohlhausen's expression [26] for flat plate may thus be used. Hence, for $N_{Pr} = 0.6$ to 15,

$$N_{St'} N_{Pr}^{2/3} = \frac{\lambda}{2} \quad (11)$$

$$\text{with } \frac{\lambda}{2} = \frac{0.664}{N_{Re}^{1/2}}$$

λ being the skin-friction drag coefficient. For the present calculation, the characteristic length in N_{Re} and N_{Nu} is taken as πa which is one-half of the circumference of a great circle of the eddy. Admittedly, such a selection as well as the model used for heat transfer and drag calculation is somewhat arbitrary. It is hoped that the major inaccuracies so introduced could be adequately

compensated by including one empirical constant in the analysis which will be described shortly.

With the foregoing characteristic length, the Reynolds and average Nusselt number of the eddy are:

$$N_{Re'} = \left(\frac{u_2 + u_1}{2} - \frac{u_1 + u'_1}{2} \right) \frac{\pi a}{\nu} = \frac{u_2 - u'_1}{2} \frac{\pi a}{\nu} \quad (12)$$

$$N_{Nu'} = \frac{h_e(\pi a)}{k} \quad (13)$$

It follows that the average Stanton number of the eddy is:

$$N_{St} = \frac{N_{Nu'}}{N_{Re'} N_{Pr}} \quad (14)$$

Equation (11) is known to be valid for relatively high N_{Pr} fluids as indicated. Since, in this paper, one is primarily concerned with heat transfer in liquid metals, it is necessary to deduce a similar expression for fluids of much smaller N_{Pr} . Using the well-known approximate procedure of solving the integral momentum and energy equation of the boundary layer, one obtains:

$$N_{St'} N_{Pr}^{1/2} = 1.64 \frac{\lambda}{2} = \frac{1.06}{N_{Re}^{1/2}} \quad (15)^\dagger$$

Of particular interest is the fact that N_{Pr} which occurs in equation (11) is raised to the power $\frac{2}{3}$ while in equation (15) it is raised to the power $\frac{1}{2}$. Inasmuch as it has not been possible to use a single expression for the Stanton number, two separate expressions for the eddy diffusivity ratio will be given.

2.1. Eddy diffusivity ratio for fluids of Prandtl number ranging from 0.6 to 15

If one introduces the Peclet number of the eddy $N_{Pe'}$ ($=N_{Re'} N_{Pr}$) into equation (8b), there results:

$$X = \left(\frac{\pi}{2N_{Pe'}} \right)^{1/2} \left(1 + \frac{N_{Nu'}}{\pi} \right) \left(\frac{l}{a} \frac{u_2 - u'_1}{v'} \right)^{1/2} \quad (16)$$

As pointed out earlier, due to the arbitrariness of the selected shape of the eddy, model for the

[†] A detailed derivation is given in [33].

heat transfer process, etc., it was decided to replace the constant 0.664 in the Pohlhausen equation by an empirical constant b , the value of which is to be determined later. Accordingly, one writes equation (11) in the modified form:

$$N_{St'} N_{Pr}^{2/3} = \frac{b}{N_{Re}^{1/2}} \quad (17)$$

Introducing this relation into equations (10) and (16) and inserting the results into equation (3), yield:

$$\frac{\epsilon_H}{\epsilon_M} = \left. \frac{1 + \frac{3}{2}b(l/a) [(u_2 - u_1')/v'] N_{Re}^{-1/2}}{1 + \frac{3}{2}\{1/[0.318N_{Pr} + (1/b)(N_{Re}^{1/2} N_{Pr}^{2/3})]\}} \left\{ \frac{(l/a) [(u_2 - u_1')/v'] + 0.203b N_{Pr}^{4/3} N_{Re}^{3/2}}{F(X)/(1 + 0.318b N_{Pr}^{1/3} N_{Re}^{1/2})^2} \right\} \right\} \quad (18)$$

in which $F(X)$ is given by equation (8a) and

$$X = \left(\frac{\pi}{2}\right)^{1/2} \left(\frac{b}{\pi N_{Pr}^{1/6}} + \frac{1}{N_{Pr}^{1/2}}\right) \left(\frac{l}{a} \frac{u_2 - u_1'}{v'}\right)^{1/2} \quad (19)$$

2.2. Eddy diffusivity ratio for liquid metals

Following the same argument expounded in the preceding section, one modifies equation (15) as

$$N_{St'} N_{Pr}^{1/2} = 1.64 \frac{b}{N_{Re}^{1/2}} \quad (20)$$

The corresponding expressions for equation (18) and (19) are, for this case,

$$\frac{\epsilon_H}{\epsilon_M} = \left. \frac{1 + \frac{3}{2}b(l/a) [(u_2 - u_1')/v'] N_{Re}^{-1/2}}{1 + \frac{3}{2}\{1/[0.318N_{Pr} + (0.609/b) N_{Pr}^{1/2}]\}} \left\{ \frac{(l/a) [(u_2 - u_1')/v'] + 0.333b N_{Pr}^{1/2} F(X)}{(1 + 0.522b N_{Pr}^{1/2})^2} \right\} \right\} \quad (21)$$

and,

$$X = \left(\frac{\pi}{2}\right)^{1/2} \left(0.522b + \frac{1}{N_{Pr}^{1/2}}\right) \left(\frac{l}{a} \frac{u_2 - u_1'}{v'}\right)^{3/2} \quad (22)$$

Equations (18) and (21) contain common unknowns, namely, the ratio of fluctuating velocities $(u_2 - u_1')/v'$, the ratio of mixing-length to radius of the eddy l/a , the Reynolds number of the eddy N_{Re} and empirical constant b . The following two sections are devoted to their discussion and evaluation.

2.3. Ratio of fluctuating velocities

Referring to Fig. 2(a), $u_2 - u_1'$ and v' are, respectively, the fluctuating velocities in the axial and radial direction. Both are complicated functions of space and time; their exact nature is not known. Customarily, they are treated on a statistical basis and expressed in terms of their root-mean square values. These two quantities are so interpreted in this paper.

Numerous experiments have been conducted by various investigators, notably Laufer [27], Reichardt [28], and Wattendorf [29], to study the structure of turbulence in two-dimensional channels. Laufer [30] also carried out one of the most detailed investigations on turbulence in fully developed pipe flow. When the ratio of either fluctuating velocity to the friction velocity $v^* [= \sqrt{(g_c \tau_w / \rho)}]$ were plotted against the dimensionless radial location y/r_w , it was found that, up to a region very close to the wall, both were almost independent of the Reynolds number. Laufer's measurements also indicate that $(u_2 - u_1')/v^*$ and v'/v^* vary almost linearly with radial location, showing an increase towards the wall till a maximum is reached in the buffer zone, followed by a rapid drop as the wall is approached. Laufer's results may be closely approximated by the following expressions:

$$\frac{u_2 - u_1'}{v^*} = 1.95 \left(1 - 0.64 \frac{y}{r_w}\right) \quad (23)$$

and
$$\frac{v'}{v^*} = 1.08 \left(1 - 0.36 \frac{y}{r_w}\right) \quad (24)$$

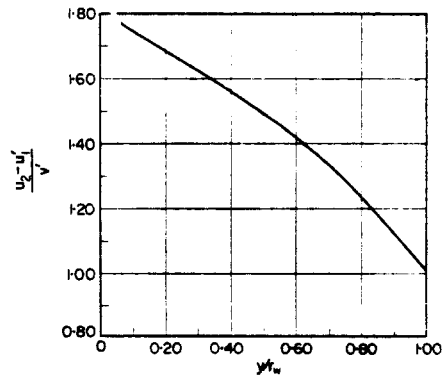


FIG. 3. Variation of fluctuating velocity ratio with radial location across pipe.

It follows that,

$$\frac{u_2 - u_1'}{v'} = 1.81 \frac{1 - 0.64 y/r_w}{1 - 0.36 y/r_w} \quad (25)$$

which is shown graphically in Fig. 3. Laufer's data were obtained for air, it will be assumed that they remain valid for other fluids.

2.4. Reynolds number of the eddy $N_{Re'}$ and the ratio l/a

Eliminating $(u_2 - u_1')$ from equations (23) and (12) gives,

$$N_{Re'} = \frac{\pi a}{2 v'} \left[1.95 v' \left(1 - 0.64 \frac{y}{r_w} \right) \right] \quad (26a)$$

which can be shown to equal

$$N_{Re'} = 1.53 \frac{a}{l} \frac{l}{r_w} \left(1 - 0.64 \frac{y}{r_w} \right) N_{Re} \sqrt{\left(\frac{f}{8} \right)} \quad (26b)$$

For $N_{Re} > 10^5$, Nikuradse [31] reported the following expression for the ratio of mixing length to pipe radius,

$$\frac{l}{r_w} = 0.14 - 0.08 \left(1 - \frac{y}{r_w} \right)^2 - 0.06 \left(1 - \frac{y}{r_w} \right)^4 \quad (27)$$

which will be extrapolated for use at lower N_{Re} since no other information is available.

Next, we shall consider the ratio l/a . In the preliminary examination of the behaviour of equation (18), the diffusivity ratio was calculated for air of $N_{Pr} = 0.718$ with the empirical constant b retained as that originally appeared in the Pohlhausen equation, namely, 0.664. Computations were carried out for $y/r_w = 0.5$ and for three arbitrarily selected values of $l/a = 2, 3$ and 4. The results are summarized in Table 1.

Table 1. Prediction of ϵ_H/ϵ_M by equation (18) for air of $N_{Pr} = 0.718$, $b = 0.664$, $y/r_w = 0.5$

N_{Re}	$\alpha = \frac{\epsilon_H}{\epsilon_M}$		
	$\frac{l}{a} = 2$	$\frac{l}{a} = 3$	$\frac{l}{a} = 4$
14,500	1.008	1.018	1.030
80,300	1.007	1.016	1.029

It is seen that the calculated ratio ϵ_H/ϵ_M is not sensitive to variations in l/a . For simplicity we select $l/a = 2$ for subsequent calculations.

Using Nikuradse's expression for l/r_w and $l/a = 2$, the Reynolds number of the eddy may be related to the pipe Reynolds number and Darcy friction factor as:

$$\frac{N_{Re'}}{N_{Re} \sqrt{(f/8)}} = 0.766 \left(1 - 0.64 \frac{y}{r_w} \right) \left[0.14 - 0.08 \left(1 - \frac{y}{r_w} \right)^2 - 0.06 \left(1 - \frac{y}{r_w} \right)^4 \right] \quad (28)$$

which is shown plotted in Fig. 4. It vanishes at the wall, reaches a maximum at about $y/r_w = 0.5$ and then decreases toward the pipe center. $N_{Re'}$ may be regarded as a measure of the turbulence intensity.

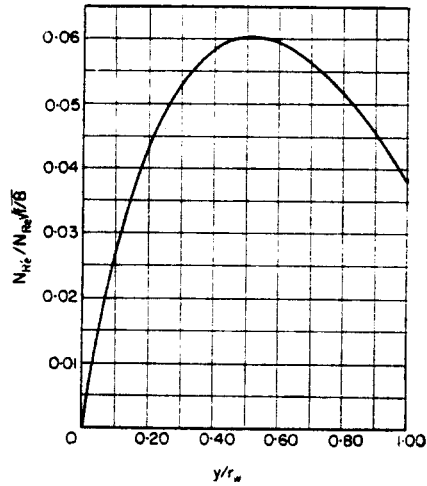


FIG. 4. Variation of $\frac{N_{Re'}}{N_{Re} \sqrt{(f/8)}}$ with radial location across pipe.

Diffusivity ratios for air as listed in Table 1 are only slightly higher than unity. Page *et al.* [18] reported experimentally determined values of α for air flowing between parallel plates. Sleicher [19] also reported data for air in turbulent pipe flow. While there are some discrepancies between Page's and Sleicher's results, the general behavior with respect to the influence of Reynolds-number and location across the pipe or channel seems to be in good agreement.

However, Sleicher's data have been chosen for the determination of the empirical constant b in equation (18) because they were obtained for pipe flow. After a few calculations, it was found that by assigning $b = 2.5$, the predicted value for air at $N_{Re} = 14,500$ and $y/r_w = 0.35$ could be made to agree with Sleicher's data. The reason for the selection of this particular y/r_w was that the experimental data indicated a nearly constant trend beyond this location. It is pertinent that the artificial matching of the theoretical equation (18) and experimental data was done at only one point and only for $N_{Pr} = 0.718$.

Using the expression for the ratio of fluctuating velocities given by equation (25), $l/a = 2$, and $b = 2.5$, equations (18) and (21) finally become:

$$\frac{\epsilon_H}{\epsilon_M} = \frac{1 + 6.77\phi N_{Re}^{-1/2}}{1 + 0.75 F_1 F_2} \quad (29)$$

in which

$$\phi = \frac{1 - 0.64 y/r_w}{1 - 0.36 y/r_w} \quad (29a)$$

and,

(i) For fluids of N_{Pr} ranging from 0.6 to 15

$$\left. \begin{aligned} F_1 &= \frac{1}{0.318 N_{Pe}' + 0.4 N_{Pe}'^{1/2} N_{Pr}^{1/6}} \\ F_2 &= 3.61\phi + \frac{0.508 N_{Pe}'^{3/2} N_{Pr}^{-1/6}}{(1 + 0.795 N_{Pe}'^{1/2} N_{Pr}^{-1/6})^2} F(X) \\ X &= 2.38\phi^{1/2} (N_{Pe}'^{-1/2} + 0.795 N_{Pr}^{-1/6}) \end{aligned} \right\} \quad (29b)$$

(ii) For liquid metals

$$\left. \begin{aligned} F_1 &= \frac{1}{0.318 N_{Pe}' + 0.244 N_{Pe}'^{1/2}} \\ F_2 &= 3.61\phi + \frac{0.833 N_{Pe}'^{3/2}}{(1 + 1.305 N_{Pe}'^{1/2})^2} F(X) \\ X &= 2.38\phi^{1/2} (1.305 + N_{Pe}'^{-1/2}) \end{aligned} \right\} \quad (29c)$$

In either case, $N_{Pe}' = N_{Re}' N_{Pr}$, N_{Re}' is given by equation (28) and $F(X)$ by equation (8a).

For approximate calculations, the following may be used:

(i) For fluids of N_{Pr} ranging from 0.6 to 15

$$\frac{\epsilon_H}{\epsilon_M} = \frac{1 + 135 N_{Re}^{-0.45} \exp[-(y/r_w)^{0.25}]}{1 + 57 N_{Re}^{-0.44} N_{Pr}^{-0.58} \exp[-(y/r_w)^{0.25}]} \quad (30a)$$

(ii) For liquid metals

$$\frac{\epsilon_H}{\epsilon_M} = \frac{1 + 135 N_{Re}^{-0.45} \exp[-(y/r_w)^{0.25}]}{1 + 380 N_{Pe}^{-0.58} \exp[-(y/r_w)^{0.25}]} \quad (30b)$$

both give a maximum deviation of less than 14 per cent.

3. COMPUTED RESULTS ON DIFFUSIVITY RATIO, α

Equations (29), (29a) and (29b) have been used to evaluate α for fluids of $N_{Pr} = 0.718, 1$ and 10 at several N_{Re} . Results obtained for $N_{Pr} = 0.718$ are plotted in Fig. 5. For purpose of comparison, Sleicher's experimental results are also shown.

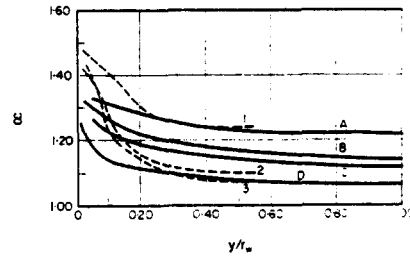


FIG. 5. Comparison of Sleicher's experimental data with calculated values of diffusivity ratio.

- $N_{Pr} = 0.718$
- Theoretical prediction
 - 1, A $N_{Re} = 1.45 \times 10^4$
 - B $N_{Re} = 4.34 \times 10^4$
 - 3, C $N_{Re} = 8.03 \times 10^4$
 - D $N_{Re} = 3.96 \times 10^5$
 - 2 $N_{Re} = 3.85 \times 10^4$
 - - - Sleicher's data.

It may be recalled that the empirical constant b in equations (18) and (21) was determined by matching the calculated value of α with Sleicher's data at only a single point. It is interesting to note that the predicted variation of α with N_{Re} and radial location does show fair agreement with experiments. While Sleicher reported values of α for y/r_w only up to 0.55, Page's data included regions close to the channel center. The latter indicate a continuous, slight decrease of α towards the channel center—a trend also revealed by the present analysis. Fig. 6 illustrates the calculated results for $N_{Pr} = 1$ and 10 . The former differs from Jenkins' prediction [22] which gives $\alpha = 1$ when $N_{Pr} = 1$ irrespective of N_{Re} . No experimental data for higher Prandtl number fluids are available for comparison.

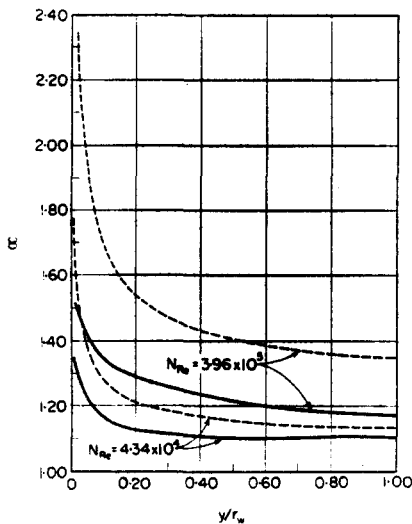


FIG. 6. Calculated variation of diffusivity ratio with radial location for two Prandtl numbers and two Reynolds numbers.

— $N_{Pr} = 1.0$ - - - $N_{Pr} = 10$.

One interesting consequence of the present analysis is that α , for any N_{Pr} , approaches unity as N_{Re} increases indefinitely. When this occurs, both the numerator and denominator of equation (29) become unity. It implies that at very high N_{Re} , the original Prandtl's mixing-length hypothesis becomes valid. At this point, a question which naturally arises is: Why does the previous analysis, such as that of von Kármán [7], Martinelli [9], or Lyon [10] in which α is assumed to be unity for all N_{Re} and N_{Pr} , give good prediction of heat transfer for fluids of N_{Pr} equal to or higher than that of air? The answer lies in the fact that, in such fluids, the thermal resistance is essentially confined to the laminar sub-layer and buffer region. For instance, at $N_{Re} = 10,000$, Martinelli [9] reported that over 99 per cent of the temperature difference occurred in the combined laminar sub-layer and buffer zone for a fluid of $N_{Pr} = 100$. The corresponding values for $N_{Pr} = 1$ and 0.01 are 71 per cent and 21 per cent, respectively. Hence, for ordinary fluids, any inaccuracy which one introduces in computing the thermal resistance of the turbulent core would have only minor effect on the prediction of Nusselt number. This is not the case for liquid metals.

It is also seen that Sleicher's data for air which showed $\alpha > 1$ at a region close to wall are not contradictory to the fact that von Kármán's analysis and others ($\alpha = 1$) give reasonably good agreement with experiment in so far as the prediction of heat transfer is concerned. In the laminar sub-layer, turbulence is, by and large, suppressed, and molecular conduction predominates.

The available experimental data of α for liquid metals are those of Isakoff and Drew [15] and Brown *et al.* [20]. Again, for the purpose of

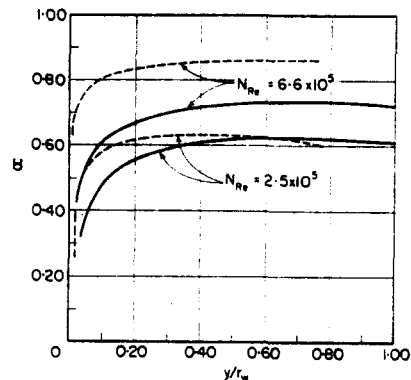


FIG. 7. Comparison of experimental data of diffusivity ratio for mercury due to Brown, Amstead and Short with calculated values.

$N_{Pr} = 0.02$

— Theoretical prediction - - - Brown *et al.*

comparison, numerical calculations of equations (29), (29a) and (29c) were carried out for $N_{Pr} = 0.0239$ and 0.02 at several N_{Re} . The two N_{Pr} selected correspond to those of mercury as reported respectively in [15] and [20]. Results of computation are shown in Figs. 7 and 8. The theoretical prediction of equations (29), (29a) and (29c) is seen to be in fair agreement with the experimental measurements of Brown. It is to be emphasized that the comparison made here involves no further matching of the empirical constant which has been previously determined from results on air. At the lower N_{Re} , the agreement is considered good. At the higher N_{Re} , the theory predicts lower values. According to the present analysis one sees that, for liquid metals, increasing N_{Re} tends to increase α , a trend which is an antithesis to that for air or higher N_{Pr}

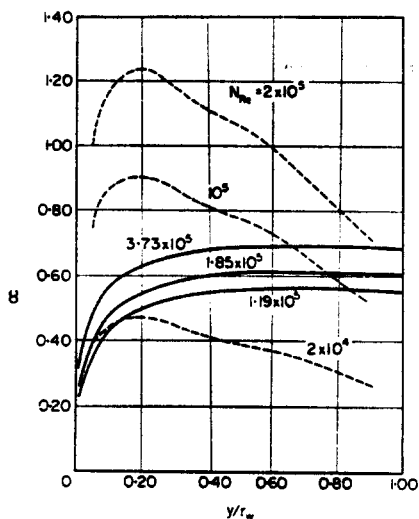


FIG. 8. Comparison of experimental data of diffusivity ratio for mercury due to Isakoff and Drew with calculated values. $N_{Pr} = 0.0239$

--- Isakoff and Drew ——— Present analysis.

fluids. Fig. 7 shows that there is a slight drop in the values of α as the center of the pipe is approached—a phenomenon which may also be noticed in Brown's data. Isakoff and Drew's results do not agree with those of Brown *et al.*, and hence are not in agreement with those pre-

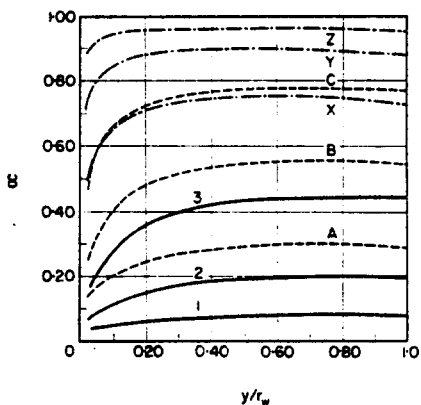


FIG. 9. Predicted variations of diffusivity ratio with radial location as influenced by Prandtl numbers and Reynolds numbers

——— $N_{Pr} = 0.001$ 1, A, X $N_{Re} = 4.34 \times 10^4$
 - - - $N_{Pr} = 0.01$ 2, B, Y $N_{Re} = 3.96 \times 10^5$
 - - - $N_{Pr} = 0.1$ 3, C, Z $N_{Re} = 3.24 \times 10^6$.

dicted by the present theory. Drew and Isakoff based their calculation on temperature data which showed considerable scatter. As will be pointed out in a later section, some of their reported temperature profiles fell below the limiting profile of $N_{Pr} = 0$. This led the writers to believe that Isakoff and Drew's results are most probably in error.

Equations (29), (29a) and (29c) have also been used to calculate for $N_{Pr} = 0.001, 0.01$ and 0.1 and for $N_{Re} = 4.34 \times 10^4, 3.96 \times 10^5$ and 3.24×10^6 . Fig. 9 summarizes the results obtained. For a given N_{Pr} , α increases with increase in N_{Re} . In the limit, as $N_{Re} \rightarrow \infty, \alpha \rightarrow 1$ for any N_{Pr} . As the distance from wall increases, α also increases, first rapidly and then slowly till it assumes a more or less constant value. For the highest Prandtl number investigated, namely 0.1, there is less variation of α with respect to radial location across the pipe, particularly when the Reynolds number is large.

4. NUSSELT NUMBER AND TEMPERATURE PROFILE FOR FULLY DEVELOPED PIPE FLOW WITH CONSTANT WALL FLUX

The case to be considered concerns the turbulent flow of liquid metals in smooth, circular pipes with constant wall flux. The fluid properties are regarded as constants. This problem was first considered by Martinelli [9] who recognized the importance of molecular conduction in the turbulent core for the transfer of heat in fluids of very low Prandtl number, such as molten metals. Martinelli's analysis was later modified by Lyon [10] who showed that the Nusselt number could be expressed as:

$$\frac{1}{N_{Nu, b}} = 2 \int_0^1 \frac{(j^* U Z dZ)^2}{Z [1 + \alpha (\epsilon_M / \nu) N_{Pr}]} dZ \quad (31)$$

In the above expression, the Nusselt number is based on temperature difference between the wall and the bulk of the fluid. Lyon integrated equation (31) numerically, using point values of velocity and ϵ_M / ν as evaluated directly from Nikuradse's data [31]. Like Martinelli, Lyon assumed that $\alpha = 1$ in his calculations. He approximated his results of calculation for

Nusselt number by the following interpolation formula:

$$N_{Nu,b} = 7 + 0.025 N_{Pr}^{0.8} \quad (32)$$

which has been recommended for use in the *Liquid Metals Handbook* [32]. The results of experiments are on the average, about 50 per cent lower than the prediction of equation (32). It is clear from equation (31) that, for a given N_{Pr} , the Nusselt number depends on α , ϵ_M/ν and the velocity profile whose effect is reflected in the integral $\int_0^z UZdZ$. The latter two quantities will be discussed separately in the following sections.

4.1. The integral $\int_0^z UZdZ$

For an incompressible fluid of constant properties flowing turbulently in a pipe with fully developed velocity and temperature profiles, Seban and Shimazaki [2] showed that, for constant wall flux, the axial temperature gradient is independent of the radial position in the pipe. Under such circumstance, it can be readily shown that the radial q -distribution is given by:

$$\frac{q}{q_w} = 2 \int_0^z UZdZ = \frac{\int_{y/r_w}^1 u^+(1 - y/r_w) d(y/r_w)}{\int_0^1 u^+(1 - y/r_w) d(y/r_w)} \quad (33)$$

If the logarithmic velocity profile proposed by von Kármán [7] were adopted, namely,

$$\left. \begin{aligned} u^+ &= y^+, & 0 \leq y^+ < 5 \\ u^+ &= -3.05 + 5 \ln y^+, & 5 \leq y^+ < 30 \\ u^+ &= 5.5 + 2.5 \ln y^+, & y^+ \geq 30 \end{aligned} \right\} (34)$$

the integrals in equation (33) could be readily evaluated and the result expressed in a closed form. It is,

$$\frac{q}{q_w} = \frac{2.75(1 - y/r_w)^2 + 1.25 \ln N_{Re}/2\sqrt{(f/8)} - 1.25y/r_w(2 - y/r_w) \ln [y/r_w N_{Re}/2\sqrt{(f/8)}] - 0.625(1 - y/r_w)(3 - y/r_w)}{1.25 \ln N_{Re}/2\sqrt{(f/8)} - 127.8(N_{Re}\sqrt{(f/8)}^{-1} + 22,960[N_{Re}\sqrt{(f/8)}]^{-2} + 0.875)} \quad (35)$$

Equation (35) ignores the influence of laminar

sub-layer and buffer region. If the latter is considered additional terms will appear in the numerator of the above equation. A detailed derivation has been given [33]. For the present analysis, equation (35) may be used for the entire cross-section without sacrificing accuracy. Fig. 10 is a graphical representation of such distribution for N_{Re} ranging from 4×10^3 to 3.24×10^6 .

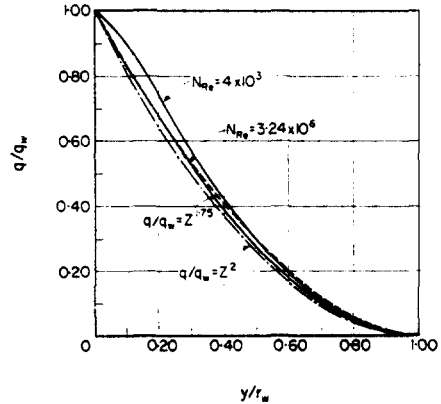


FIG. 10. Radial q -distribution in fully developed turbulent pipe flow.

— q -distribution according to equation (35)
 - - - Martinelli's distribution
 . . . Simple distribution used in the present analysis.

These correspond to the extremes of N_{Re} used by Lyon. Calculated data for all intermediate N_{Re} lie within the narrow loop bounded by the two solid curves. It is thus seen that for the realm of N_{Re} considered, the ratio q/q_w may be closely approximated by a single curve expressible by:

$$\frac{q}{q_w} = 2 \int_0^z UZdZ \simeq \left(1 - \frac{y}{r_w}\right)^{1.75} = Z^{1.75} \quad (35a)$$

Lyon's individually computed values agree well with this simple result. This is demonstrated in Table 2.

That the q -distribution in turbulent pipe flow is insensitive to Reynolds number variation has also been confirmed experimentally by Isakoff [34].

With the foregoing simplification, equation (31) could be written as:

$$\frac{1}{N_{Nu,b}} = \frac{1}{2} \int_0^1 \frac{Z^{2.5}}{1 + (\alpha \epsilon_M/\nu) N_{Pr}} dZ \quad (36)$$

Table 2. Comparison of the numerical values of the integral $\int_0^z ZUdZ$ as reported by Lyon and the suggested relation given by equation (35a)

$\frac{y}{r_w}$	Z	$\int_0^z ZUdZ$ due to Lyon			$\frac{Z^{1.75}}{2}$
		$N_{Re} = 4.34 \times 10^4$	$N_{Re} = 3.96 \times 10^5$	$N_{Re} = 3.24 \times 10^6$	
0	1	0.5022	0.4990	0.5004	0.5000
0.1	0.9	0.4287	0.4230	0.4216	0.4158
0.2	0.8	0.3490	0.3430	0.3405	0.3384
0.3	0.7	0.2735	0.2680	0.2651	0.2679
0.4	0.6	0.2047	0.2000	0.1974	0.2045
0.5	0.5	0.1444	0.1410	0.1386	0.1487
0.6	0.4	0.0936	0.0909	0.0895	0.1006
0.7	0.3	0.0532	0.0515	0.0508	0.0608
0.8	0.2	0.0238	0.0230	0.0228	0.0299
0.9	0.1	0.0060	0.0058	0.0057	0.0089
1.0	0	0	0	0	0

It is interesting to note that the corresponding expression used by Martinelli has the exponent of Z replaced by 3, since the rather crude assumption $u = u_b$, was adopted in his analysis.

4.2. The ratio of eddy viscosity to kinematic viscosity, ϵ_M/ν

A rational calculation of the ratio ϵ_M/ν is not possible at the present time since no precise theory of turbulence exists. Consequently, one turns to experimentally measured velocity profile for the evaluation of ϵ_M . After examining the several turbulent velocity profiles proposed by various investigators, namely, Prandtl [35] von Kármán [36], Deissler [37] Reichardt [38] Rannie [39] Ross [40] and Pai [41], the writers came to the following conclusion. The semi-empirical velocity profiles proposed by various investigators may seemingly fit well the experimental data, it does not necessarily follow that the assumed model of turbulence is precise. ϵ_M calculated from the directly measured velocity gradient across the pipe may not be in good agreement with that computed from the semi-empirical equation which is supposedly to represent the velocity distribution. A detailed analysis and discussion is given in [33]. For fluids of relatively high N_{Pr} , any error introduced in the evaluation of ϵ_M will produce only minor effect on the final result of Nusselt number calculations. This is no longer true for liquid

metals. In view of these observations, it was decided to use Nikuradse's data of ϵ_M/ν [31] which were evaluated directly from the measured velocity gradient. However, no data were reported by Nikuradse for $y/r_w < 0.02$. Extrapolation was then made with the aid of Kármán profile as given by equation (34). For those cases of N_{Re} for which no information was reported by Nikuradse, Deissler's velocity profile [37] has been used for the determination of ϵ_M .

4.3. Result of Nusselt number calculations

With α and ϵ_M/ν known, the Nusselt number may be evaluated from equation (36), using numerical integration. For the purpose of comparison, the Prandtl and Reynolds number selected were those used by Lyon, i.e. $N_{Pr} = 0, 0.001, 0.01, \text{ and } 0.1$ and $N_{Re} = 4.34 \times 10^4, 3.96 \times 10^5 \text{ and } 3.24 \times 10^6$. For the limiting case of $N_{Pr} = 0$, equation (36) may be readily integrated to give $N_{Nu, b} = 7$. This limiting Nusselt number is independent of the Reynolds number, at least for the range considered in the present work. As $N_{Re} \rightarrow \infty$, the flux distribution becomes linear which has been assumed by Martinelli. Consequently, the exponent of Z in equation (36) should be replaced by 3, which gives a limiting value of 8 as $N_{Pr} \rightarrow 0$.

Calculated values of Nusselt number for the four N_{Pr} and three N_{Re} selected are listed in Table 3. Tabulated also are the results reported

Table 3. Calculated values of Nusselt number

N_{Re}	N_{Pr}	N_{Pe}	$N_{Nu,b}$	
			Lyon's theoretical result	Present theory equation (36)
4.34×10^4	0	0	6.83	7
	0.001	43.4	7.30	7.04
	0.01	434	10.30	8.01
	0.1	4340	30.5	26.07
3.96×10^5	0	0	7.05	7
	0.001	396	9.54	7.46
	0.01	3960	26.5	16.9
	0.1	39,600	132.0	108
3.24×10^4	0	0	7.17	7
	0.001	3240	20.8	12.5
	0.01	32,400	100	65.2

by Lyon. A significant difference is seen to exist. For design computations, Lyon approximated his calculated results by equation (32) with a maximum deviation of 12 per cent. Lyon's expression implies that viscosity has no effect on turbulent heat transfer in liquid metals. This, however, can not be confirmed by the present results. Fig. 11 illustrates the independent effect of Prandtl and Reynolds number on the Nusselt number. For $N_{Pr} < 0.1$, and $N_{Pe} < 15,000$, the theoretical results of the present analysis could

be represented by an interpolation formula of the form:

$$N_{Nu,b} = 7 + 0.05 N_{Pe}^{0.77} N_{Pr}^{0.25} \quad (37)$$

which gives a maximum deviation of less than 12 per cent.

To ascertain the accuracy of equation (37), some of Lubarsky and Kaufman's re-evaluated experimental data on mercury and lead-bismuth eutectic [1] were reproduced in Figs. 12(a, b, c)

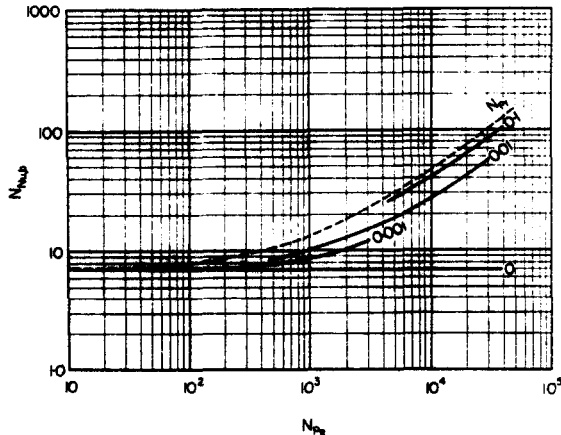


FIG. 11. Comparison of Lyon's equation and the predicted Nusselt numbers according to the present analysis.
 — — — Lyon's equation $N_{Nu,b} = 7 + 0.025 N_{Pe}^{0.6}$.

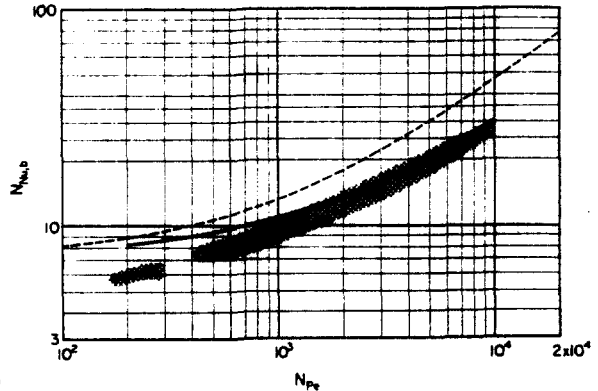


FIG. 12(a). Comparison of experimental Nusselt number for mercury due to Johnson, Clabaugh and Hartnett [1] with the present analysis.
 $N_{Pr} = 0.022$
 - - - Lyon
 — — — Present analysis, equation (37).

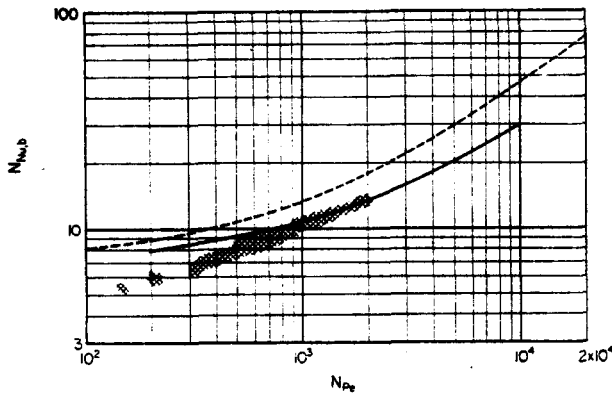


FIG. 12(b). Comparison of experimental Nusselt number for mercury due to Trefthen [1] with the present analysis.

$$N_{Pr} = 0.02$$

--- Lyon
 — Present analysis, equation (37).

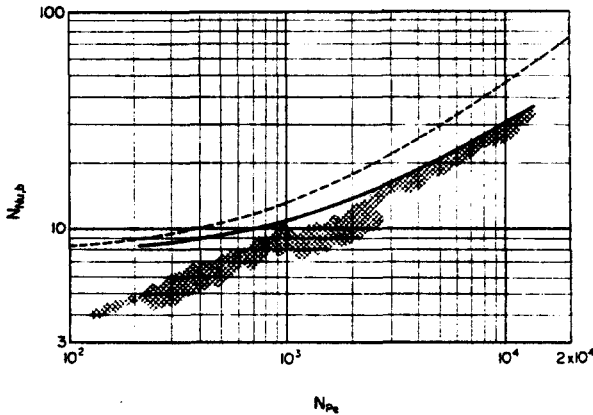


FIG. 12(c). Comparison of experimental Nusselt number for mercury due to Stromquist [1] with the present analysis.

$$N_{Pr} = 0.02$$

--- Lyon
 — Present analysis, equation (37).

and Figs. 13(a, b). Comparison is made to those predicted by equation (37) as well as to those of Lyon. The improvement over Lyon's expression is obvious. However, according to the proposed theory, the lowest possible Nusselt number is 7 but the bulk of experimental data at low Peclet numbers indicate a value considerably less than 7. It is not clear at the present time whether this indicates a deficit in the theory or is due to errors in experimental data. In a dis-

cussion of [24], Lyon pointed out that since most of the data in this range of N_{Pe} were obtained in a horizontal tube with dense fluids (mercury and lead-bismuth), the stratifying effect of thermal expansion might have been the cause.

Having carefully examined published data on liquid metal heat transfer, Lubarsky and Kaufman [1] proposed an empirical equation of the form:

$$N_{Nu, b} = 0.625 N_{Pe}^{0.4} \quad (38)$$

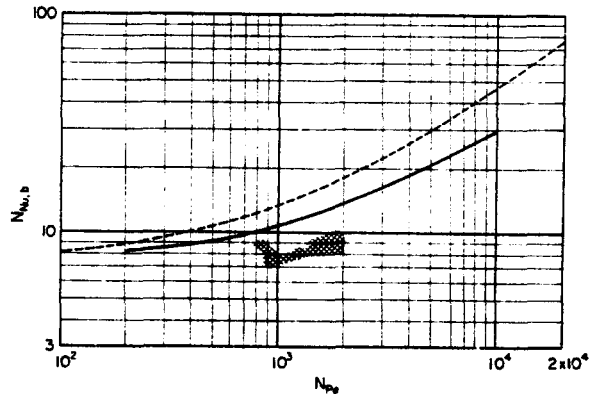


FIG. 13(a). Comparison of experimental Nusselt number for lead-bismuth eutectic due to Seban [1] with the present analysis.

$$N_{Pr} = 0.02$$

--- Lyon
 — Present analysis, equation (37).

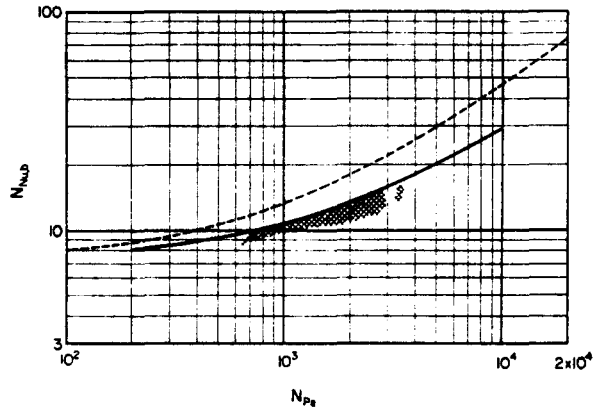


FIG. 13(b). Comparison of experimental Nusselt number for lead-bismuth eutectic due to Johnson, Hartnett and Clabaugh [1] with the present analysis.

$$N_{Pr} = 0.023$$

--- Lyon
 — Present analysis, equation (37).

which has been claimed to best fit most of the fully developed turbulent heat transfer data on liquid metals. It is shown plotted in Fig. 14 along with the theoretical relation depicted by equation (37). Like Lyon's expression, equation (38) does not involve viscosity. At the present

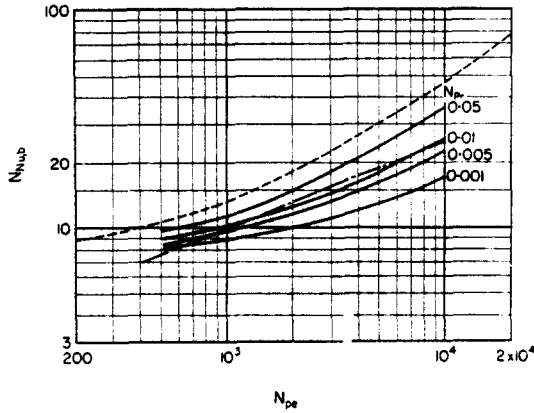


FIG. 14. Comparison of Lyon's theoretical prediction, the empirical relation due to Lubarsky and Kaufman with the present analysis.

- Lyon $N_{Nu,b} = 7 + 0.025 N_{Pe}^{0.8}$
- Present analysis $N_{Nu,b} = 7 + 0.05 N_{Pe}^{0.77} N_{Pr}^{0.28}$
- - - Lubarsky and Kaufman $N_{Nu,b} = 0.625 N_{Pe}^{0.4}$.

time, experimental data are not available to confirm or to contradict the independent effect of N_{Pr} as indicated by equation (37).

4.4. Temperature profile

If the dimensionless variable Z is introduced into equation (2), followed by using the q -distribution given by equation (35a), one obtains, upon integration,

$$t_w - t = \frac{q_w r_w}{A_w k} \int_z^1 \frac{Z^{0.75}}{1 + \alpha(\epsilon_M/\nu) N_{Pr}} dZ \quad (39)$$

Hence, the normalized temperature profile is

$$\frac{t_w - t}{t_w - t_c} = \frac{\int_z^1 \{Z^{0.75} dZ / [1 + \alpha(\epsilon_M/\nu) N_{Pr}]\}}{\int_0^1 \{Z^{0.75} dZ / [1 + \alpha(\epsilon_M/\nu) N_{Pr}]\}} \quad (40)$$

For the limiting case of vanishingly small Prandtl number, but finite N_{Re} , equation (40) reduces to a simple form:

$$\frac{t_w - t}{t_w - t_c} = 1 - Z^{1.75} \quad (41)$$

which is independent of the Reynolds number, at least for the range considered in this paper. An interesting corollary is: For a fluid of very low N_{Pr} , say 0.001 or less, one might expect that the influence of N_{Re} on both temperature profile and $N_{Nu,b}$ would be small.

On the other hand as $N_{Pe} \rightarrow \infty$, the velocity profile becomes flat, and the heat flux (q/A) distribution becomes linear. The temperature distribution is then given by:

$$\frac{t_w - t}{t_w - t_c} = \frac{\int_z^1 \{Z dZ / [1 + \alpha(\epsilon_M/\nu) N_{Pr}]\}}{\int_0^1 \{Z dZ / [1 + \alpha(\epsilon_M/\nu) N_{Pr}]\}} \quad (42)$$

which has been indiscriminately used by Martinelli [9] for all N_{Re} . If, furthermore, the condition $N_{Pr} \rightarrow 0$ is introduced into equation (42), there results,

$$\frac{t_w - t}{t_w - t_c} = 1 - Z^2 \quad (43)$$

which is a parabolic distribution.

Several temperature profiles have been calculated by numerical integration for the following cases for which experimental data are available for comparison: (i) Mercury of $N_{Pr} = 0.0239$; $N_{Pe} = 1.19 \times 10^6$ and 3.73×10^6 . Data reported by Isakoff and Drew [15]. (ii) Mercury of $N_{Pr} = 0.02$; $N_{Re} = 2.5 \times 10^5$ and 6.6×10^5 . Data reported by Brown *et al.* [20]. Results of computation are shown plotted in Figs. 15(a, b)

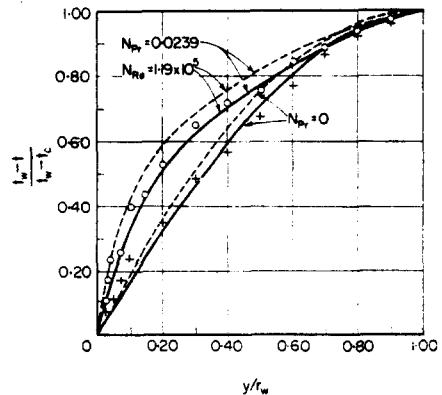


FIG. 15(a). Comparison of measured temperature distribution in mercury by Isakoff and Drew [15] with calculated profiles.

- Isakoff and Drew $N_{Re} = 1.19 \times 10^6$
- + Isakoff and Drew $N_{Re} = 4.73 \times 10^4$
- - - Martinelli
- Present analysis.

and Figs. 16(a, b). Included are Martinelli's theoretical predictions. In general, Martinelli's profile exhibits a steeper temperature change at the wall vicinity than that predicted by the present theory. This is to be expected since Martinelli's analysis predicts Nusselt numbers which are too high. From the plotted results, it is seen that the temperature profile as calculated from equation (40) has somewhat better agreement with measured data than Martinelli's prediction. The difference, however, is not great.

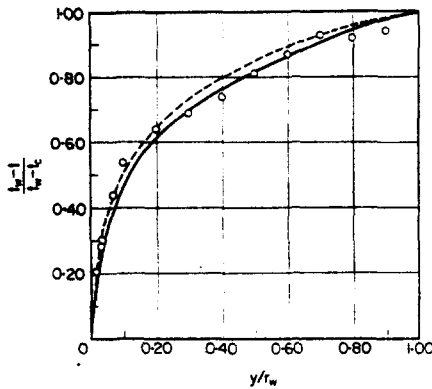


FIG. 15(b). Comparison of measured temperature distribution in mercury by Isakoff and Drew [15] with the calculated profile.

○ Isakoff and Drew $N_{Pr} = 0.0239$, $N_{Re} = 3.73 \times 10^5$
 - - - Martinelli
 — Present analysis.

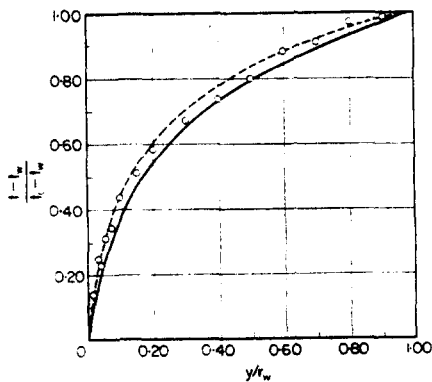


FIG. 16(a) Comparison of measured temperature distribution in mercury by Brown, Amstead and Short [20] with the calculated profile.

○ Brown *et al.* $N_{Pr} = 0.02$, $N_{Re} = 2.5 \times 10^5$
 - - - Martinelli
 — Present analysis.

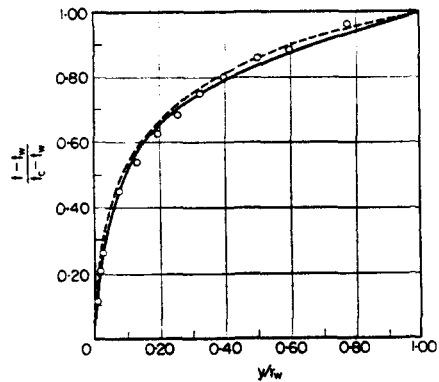


FIG. 16(b). Comparison of measured temperature distribution in mercury by Brown, Amstead and Short [20] with the calculated profile.

○ Brown *et al.* $N_{Pr} = 0.02$, $N_{Re} = 6.6 \times 10^5$
 - - - Martinelli
 — Present analysis.

In a discussion of a recent paper [24], Sleicher pointed out that normalization of temperature profiles often made it inadequate for comparison.

It should be mentioned that the experimental data of Isakoff and Drew exhibit, in many cases, considerable scatter. Many of their data for $N_{Re} = 4.73 \times 10^4$ fell below the limiting profile of $N_{Pr} = 0$ as shown in Fig. 15(a), which is most unlikely. As pointed out earlier, this consideration made the writers doubt seriously the accuracy of the α -values reported by Isakoff and Drew. In general, Brown's data had less scatter and showed much better agreement with the theoretical results.

Computed results on Nusselt number and temperature profile in fully developed pipe flow with constant wall temperature will be given in a subsequent paper.

REFERENCES

1. B. LUBARSKY and S. J. KAUFMAN, *Review of Experimental Investigations of Liquid Metal Heat Transfer*. NACA Report 1270 (1956); NACA TN 3336 (1955).
2. R. A. SEBAN and T. T. SHIMAZAKI, *Trans. Amer. Soc. Mech. Engrs.* 73, 803 (1951).
3. P. SCHNEIDER, *Effect of Axial Conduction on Heat Transfer in the Entrance Regions of Parallel Plates and Tubes*. Heat Transfer and Fluid Mechanics Institute, Preprints of Papers, Stanford University, p. 41 (1956).
4. O. REYNOLDS, *Proc. Manchr. Lit. Philos. Soc.* 14, 7 (1874).

5. G. I. TAYLOR, *Conditions at the Surface of a Hot Body Exposed to Wind*. Technical Report of the Advisory Committee for Aeronautics, Vol. 2; Reports and Memo no. 272, 423 (1916).
6. L. PRANDTL, *Phys. Z.* **29**, 487 (1928).
7. T. VON KÁRMÁN, *Trans. Amer. Soc. Mech. Engrs.* **61**, 705 (1939).
8. R. C. MARTINELLI, L. M. K. BOELTER and F. JONNASSEN, *Trans. Amer. Soc. Mech. Engrs.* **63**, 447 (1941).
9. R. C. MARTINELLI, *Trans. Amer. Soc. Mech. Engrs.* **69**, 947 (1949).
10. R. N. LYON, *Chem. Engng. Progr.* **47**, 75 (1951).
11. R. G. DESSLER, *Analytical Investigation of Turbulent Flow in Smooth Pipes with Heat Transfer with Variable Fluid Properties for Prandtl Number of 1*. NACA TN 2242 (1950).
12. R. G. DESSLER and C. S. EIAN, *Analytical and Experimental Investigation of Fully Developed Turbulent Flow of Air in a Smooth Tube with Heat Transfer with Variable Fluid Properties*. NACA TN 2629 (1952).
13. W. A. SHEPPARD, MS Thesis, Mech. Eng. Dept., University of California (1946).
14. W. H. CORCORAN, B. ROUBUSH and B. H. SAGE, *Chem. Engng. Progr.* **43**, 135 (1947).
15. S. E. ISAKOFF and T. B. DREW, *General Discussion on Heat Transfer* p. 405. Institution of Mechanical Engineers, London (1951).
16. R. A. SEBAN and T. T. SHIMAZAKI, *General Discussion on Heat Transfer* p. 122. Institution of Mechanical Engineers, London (1951).
17. W. H. CORCORAN, F. PAGE, W. G. SCHLINGER and B. H. SAGE, *Industr. Engng. Chem.* **44**, 410 (1952).
18. F. PAGE, W. G. SCHLINGER, D. K. BREAUX and B. H. SAGE, *Industr. Engng. Chem.* **44**, 424 (1952).
19. C. A. SLEICHER, JR., Ph.D. Thesis in Chemical Engineering, University of Michigan (1955); *Trans. Amer. Soc. Mech. Engrs.* **80**, 693 (1958).
20. H. E. BROWN, B. H. AMSTEAD and B. E. SHORT, *Trans. Amer. Soc. Mech. Engrs.* **79**, 279 (1957).
21. H. LUDWIG, *Z. Flugwiss.* **4**, 73 (1956).
22. R. JENKINS, *Variation of Eddy Conductivity with Prandtl Modulus and its use in Prediction of Turbulent Heat Transfer Coefficients*. Heat Transfer and Fluid Mechanics Institute, Preprints of Stanford University, p. 147 (1951).
23. R. G. DESSLER, *Analysis of Fully Developed Turbulent Heat Transfer at Low Peclet Numbers in Smooth Tubes with Application to Liquid Metals*. NACA RM E52F05 (1952).
24. P. S. LYKOUKIS and Y. S. TOULOUKIAN, *Trans. Amer. Soc. Mech. Engrs.* **653** (1958); P. S. LYKOUKIS, *Analytical Study of Heat Transfer in Liquid Metals*. Ph.D. Thesis, School of Mechanical Engineering, Purdue University (1956).
25. L. PRANDTL, *Z. angew. Math. Mech.* **5**, 136 (1925); NACA TM 1231 (1949).
26. E. POHLHAUSEN, *Z. angew. Math. Mech.* **1**, 115 (1921).
27. J. LAUFER, *Investigation of Turbulent Flow in a Two-Dimensional Channel*. NACA Rept. 1053 (1951).
28. H. REICHARDT, *Z. angew. Math. Mech.* **13**, 177 (1933); *ibid.* **18**, 358 (1938).
29. F. L. WATTENDORF, *J. Aero. Sci.* **13**, 200 (1936).
30. J. LAUFER, *The Structure of Turbulence in Fully Developed Pipe Flow*. NACA TN 2954 (1953).
31. J. NIKURADSE, *Ver. dtsh. Ing. Forsch.* **356** (1932).
32. R. LYON (Editor) *Liquid-Metals Handbook* (2nd Ed.). USAEC (1952).
33. N. Z. AZER, Ph.D. Thesis, University of Illinois (1959).
34. S. E. ISAKOFF, Ph.D. Thesis, Columbia University (1952).
35. L. PRANDTL, *Ergebnisse der Aerodynamischen Versuchsanstalt zu Göttingen*, III series (1927).
36. T. VON KÁRMÁN, *Mechanical Similitude and Turbulence*. NACA TM 611 (1931).
37. R. G. DESSLER, *Analytical and Experimental Investigation of Adiabatic Turbulent Flow in Smooth Tubes*. NACA TN 2138 (1950).
38. H. REICHARDT, *Z. angew. Math. Mech.* **31**, 208 (1951).
39. W. D. RANNIE, Ph.D. Thesis, California Institute of Technology (1951).
40. D. ROSS, *Proceedings of the Third Midwestern Conference of Fluid Mechanics*. University of Minnesota (1953).
41. S. I. PAI, *J. Franklin Inst.* **25b**, 337 (1953).